JOURNAL OF Materials CHEMISTRY

Sol–gel derived, magnesium based ionically conducting composites

Sagar Mitra and Srinivasan Sampath*

Department of Inorganic and Physical Chemistry, Indian Institute of Science, Bangalore 560 012, India. E-mail: sampath@ipc.iisc.ernet.in

Received 12th February 2002, Accepted 1st May 2002
First published as an Advance Article on the web 6th June 2002

Composite ionic conductors based on magnesium salts and sol–gel derived silicate–tetraethylene glycol hybrids have been synthesized. The structure of these materials has been studied by FT-IR, FT-Raman, ^{29}Si and ^{13}C NMR and XRD techniques. The composite systems can be best described as diphasic with silicate as fillers in the organic phase that provides solubility of the ionic dispersants. The ionic interactions in the matrix are clearly observed in the FT-Raman spectra. The ionic conductivity is determined to be of the order of 10^{-7} to 10^{-5} S cm^{-1} at room temperature for $MgCl_2$ and $Mg(ClO_4)_2$ salts respectively. The conductivity reaches 10^{-4} and 10^{-3} S cm^{-1} at 80 °C respectively.

Introduction

Magnesium based energy devices have attracted attention due to the element's relative abundance, low equivalent weight (12 g F^{-1}), low toxicity, low price and the ease of safe handling under ambient conditions.[1] Rechargeable batteries based on magnesium have important advantages over other available rechargeable systems in terms of environmental considerations. Among the few studies reported so far on the cathode materials,[1–3] an interesting recent work by Aurbach and co-workers[3] has demonstrated the use of $Mg_xMo_3S_4$ in developing a practical, rechargeable magnesium based battery. As for the electrolytes, aqueous systems do not pass the test because of the high negative potential of Mg. Other non-aqueous systems that have been studied include organomagnesium compounds in ethers or tertiary amines[1] and magnesium organohaloaluminate in tetrahydrofuran.[3] There have been some studies on the solid polymer electrolytes based on magnesium salts.[4–13] Polymeric gels together with aprotic solvents have been recently proposed as good magnesium ionic conductors[7] showing ionic conductivities of the order of 10^{-3} S cm^{-1} at 25 °C. The liquid electrolyte immobilized in the matrix is responsible for conductivity. However, the gel electrolytes do not assure a homogeneous solid phase over a wide temperature range, and have poor mechanical and thermal stability. Hence, it is desirable to have ionically conducting electrolytes consisting of a relatively rigid matrix along with a plasticizer for flexibility. The electrolyte should also exhibit good thermal and mechanical stability.

Sol–gel processing of materials leading to ionically conducting glasses has been the subject of intense study in recent years.[14–20] Mixed organic–inorganic networks based on silicate have been reported as matrices for lithium salts to achieve lithium ion conductivity.[21] The amorphous nature required for ionic conduction in this type of electrolyte is guaranteed by the presence of inorganic components.[15,22,23] Addition of fine particles to a polymer is one of the common methods of improving conductivity, amorphous domains, mechanical and thermal stability.[24] At a microscopic level, these materials are considered as 'biphasic' where the mixture is at the atomic level.[25,26] The inorganic phases can be finely dispersed using sol–gel process since the reaction is initiated using molecular precursors. Moreover, the properties of sol–gel derived composite materials are unique and different from the individual phases. The linkage between inorganic and organic phases may be based on weak interactions such as hydrogen, van der Waal's, ionic or strong chemical bonds such as covalent or iono-covalent bonds.[27] A careful examination of the literature reveals that there is no study on magnesium based ionic conductors using sol–gel derived matrices. Sol–gel processing of magnesium based solid electrolytes may yield materials with good stability coupled with good conductivity as in the case of lithium. Additionally, the recent interest in magnesium-based devices[3] prompted us to undertake this study.

Here, we report on the preparation of solid ionic conductors based on modified silicate and magnesium salts having different anions. A combination of tetraalkoxysilane and ethylene glycol that is a monomer unit for polyethylene oxide (PEO) is used in the present study. The polymerized silicate is expected to give the effect of filler in a flexible, polymer matrix. The properties of the modified silicate containing magnesium ions have been elucidated using a variety of spectroscopic techniques such as ^{29}Si, ^{13}C solid state NMR, FT-IR and FT-Raman spectroscopy. The crystallinity of the matrix is followed by X-ray diffraction (XRD) measurements. Complex impedance spectroscopy is carried out to determine the ionic conductivity at different temperatures.

Experimental section

Materials

Tetraethoxysilane (TEOS), tetraethylene glycol [$(PEG)_4$], magnesium chloride ($MgCl_2$), magnesium perchlorate [$Mg(ClO_4)_2$] and potassium bromide (KBr) were the products of Aldrich, USA. Other chemicals were from S.D Fine Chemicals, India. Double distilled water was used in all the preparations.

Synthesis

The preparation of the matrix was based on the procedure to synthesize silicate networks containing ethylene oxide functionalities.[15,25] Briefly, the preparation involved the addition of TEOS (6.5 g/6.96 mL) to PEG (4.68 g/4.17 mL) and water (1.4 mL) with vigorous stirring. The mixture was heated to 60 °C for 5 min. A calculated amount of magnesium salt (1.59 g for 0.62 M in the case of $MgCl_2$ and 1.74 g for 0.6 M for [$Mg(ClO_4)_2$] was then added and dissolved in the mixture. One drop of concentrated HCl was added to the turbid solution to catalyze the hydrolysis of the silane and the mixture was further vigorously stirred. After 10–15 minutes, the hydrolysis was completed and a single-phase solution was obtained. The mixture was then cast on a polypropylene petridish and kept in

This journal is © The Royal Society of Chemistry 2002

a vacuum oven at a temperature of 40°C for three months. Final curing of the cast and dried samples was carried out by slowly heating the samples from 60 to 90 °C over a period of three days and then keeping at 60 °C for two days. The amounts given above correspond to a $[0.5]_4[4]$ composition where the molar composition of {[PEG]/TEOS} = 0.5 and {TEOS/Mg^{+2}} = 4. The ormosils prepared are denoted by the nomenclature $[X]_n[Y]$, where $[X]$ represents the molar ratio of [PEG]/[TEOS], n is chain length of the poly(ethylene glycol) unit and $[Y]$ is the molar ratio of [TEOS]/[M^{n+}]. The samples were found to be transparent and mechanically stable, crack-free monoliths. Different series of samples were prepared and in each of these series only one of the parameters was varied (X or Y) while the other remained constant.

Experimental techniques

Vibrational spectroscopy. Infrared spectra were obtained using a Bruker Equinox-55 FT-IR spectrometer. The samples were vacuum dried at 70 °C for several days before the experiment. Raman spectra were recorded on a Bruker RFS-100/S FT-Raman spectrometer. The laser power used was 200 mW with a radiation spot of 0.1 mm diameter. The wavelength of the excitation signal was 1.064 μm (Nd : YAG laser). The scattered light was collected at an angle of 180 degree to the incident light. Each spectrum was averaged over 500 scans and the resolution was 4 cm^{-1}. A liquid nitrogen cooled germanium detector was used.

XRD. X-Ray powder data were collected using a STOE/STADI-P X-ray powder diffractometer with Cu $K\alpha_1$ (λ = 1.54 Å) radiation.

NMR. Solid-state NMR spectra were obtained on a DSX-300 Bruker spectrometer at 27 °C. Magic angle spinning NMR measurements were carried out with dried powder samples, packed into the sample holder. The spectrometer was operated at 300 MHz using magic angle spinning at a rate of 2 KHz. One-dimensional ^{13}C and ^{29}Si spectra were recorded with both cross polarization and single pulse excitation. ^{13}C spectra were recorded at a resonance frequency of 75.4 MHz and a spinning speed of 6 KHz with a cross-polarization time of 1 ms. Glycine was used as the internal reference. For ^{29}Si spectra, the resonance frequency used was 59.6 MHz with a spinning speed of 5.7 KHz.

Impedance measurements. Impedance measurements were carried out using a potentiostat/galvanostat (263 A, EG&G, NJ) coupled with a lock-in amplifier (EC-5210, EG&G, NJ) or using an electrochemical workstation (CH 660A, CH Instruments, TX). The studies have been carried out in the temperature range 25 to 80 °C and the frequency range used was between 10^5 and 0.1 Hz with an applied DC bias of 50 mV. The samples were monoliths of thickness ranging between 0.5 and 1 mm. The electrical contact between the sample and the symmetric stainless steel disc electrodes (area 0.502 cm^2) were achieved using conductive silver paste (Eltecks Corporation, India). Before the impedance measurements, all the samples were kept at 80 °C under vacuum for 7 days to remove the residual solvent and water. Prior to initiating the measurements, the samples were heated in a dynamic vacuum at 100 °C for 3 h.

Results and discussion

Table 1 shows the different compositions of the silicate-PEG materials that have been prepared in the present study. Different ratios of PEG to TEOS (X) varying from 0.5 to 2.5 and [TEOS] to [M^{n+}] (Y) varying from 80 to 2 are used to prepare the monoliths. Both $MgCl_2$ and $Mg(ClO_4)_2$ salts yield transparent and stable monoliths at all compositions except when the salt concentration is high leading to a Y ratio of 2 and the X being larger than 0.5. At this composition, the salts precipitate out leading to a two-phase mixture. Ethylene glycols with chain lengths higher than four monomeric (tetraethylene glycol) units lead to a gummy mass and the dimensional stability is reported to be very poor.[15] Hence, the study is restricted to the use of tetraethylene glycol.

Table 1 Ormocer compositions prepared in the present study. The nomenclature is $[X]_n[Y]$ where X and Y are molar ratios of [PEG]/[TEOS] and [TEOS]/M^{n+} respectively

Compositions	Salt	Compositions	Salt
$[0.5]_4[0]$		$[1]_4[80]$	
$[0.5]_4[30]$		$[1]_4[30]$	
$[0.5]_4[15]$		$[1]_4[15]$	
$[0.5]_4[8]$		$[1]_4[8]$	
$[0.5]_4[4]$		$[1]_4[4]$	
$[0.5]_4[2]$	$MgCl_2$		
		$[1.5]_4[80]$	
$[1.5]_4[0]$		$[1.5]_4[50]$	
$[1.5]_4[30]$		$[1.5]_4[20]$	
$[1.5]_4[15]$		$[1.5]_4[15]$	$Mg(ClO_4)_2$
$[1.5]_4[8]$		$[1.5]_4[8]$	
$[1.5]_4[4]$		$[1.5]_4[6]$	
$[1.5]_4[2]$		$[1.5]_4[5]$	
		$[2.5]_4[80]$	
		$[2.5]_4[30]$	
		$[2.5]_4[15]$	
		$[2.5]_4[8]$	
		$[2.5]_4[4]$	

Vibrational spectroscopy is a good tool to follow various ionic interactions in solid polymer electrolytes. Magnesium salt incorporation into PEO is expected to produce coordination compounds, as observed in the case of lithium salts, with the coordination being favored with the use of large sizes of anions.[28] The magnesium salts that are used in the present study are magnesium chloride and magnesium perchlorate and the dimensions of the anions are substantially different. Chloride has an ionic radius of 167 pm and the perchlorate anion is 236 pm in size.[11] The lattice energy is higher for magnesium chloride than that for magnesium perchlorate. This might result in the greater dissociation of the perchlorate salt compared to the chloride salt. Consequently, it may be expected that there will be a larger number of cations coordinating with the ethylene oxide unit of the matrix in the case of $Mg(ClO_4)_2$ than in the case of $MgCl_2$.

IR spectroscopy

The broad IR modes for the sol–gel silicate generally prevent a clear analysis of the IR spectra[15] in the present case. Fig. 1 shows the FT-IR spectra of as-prepared $Mg(ClO_4)_2$ incorporated PEG-silicate monolith, herein after referred to as 'ormolyte', at different conditions of vacuum drying. The absence of bands that are characteristic of ethoxy groups (around 1190, 1056 cm^{-1}) indicates that the polymerization of the silane is complete. The presence of a predominant band at around 1080 cm^{-1} is characteristic of the formation of a linear siloxane network (Si–O–Si) as reported by Buining and co-workers.[29] The band at around 1650 cm^{-1} may be attributed to a combined effect of bonding of a water molecule with an Mg^{2+} ion through the $Mg^{2+}\cdots OH_2$ and also with an ethereal oxygen of PEG through H–O–H···0 (PEG) bonding.[30] It is reported that the small dimension of magnesium ions (0.78 Å) may be unfavourable to directly bind with the ethylene oxide units that would not be sufficiently flexible to offer the ethereal oxygen atoms to the coordination sites of the metal ion. It is probably reasonable to assume that the interaction of tetraethylene glycol with the metal ion is through water molecules as given.[30]

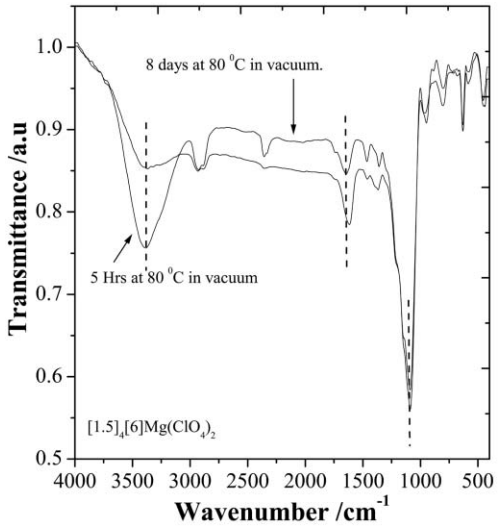

Fig. 1 FT-IR spectra of $[1.5]_4[6]Mg(ClO_4)_2$ composition in the spectral region of 4000–400 cm^{-1} at 25 °C for two different drying conditions.

As seen from the band around 3400 cm^{-1}, the intensity of O–H stretch decreases as the sample is treated under vacuum at an elevated temperature. The small peak observed at 3400 cm^{-1} after heat treatment could be due to the uncondensed silanol O–H groups and the chemically bound water molecules as shown above. The loosely bound water molecules could be removed almost completely as observed in the conductivity measurements (shown later).

FT-Raman spectroscopy

FT-Raman scattering measurements can give valuable information on the ionic interactions within the matrix. The low frequency range in the Raman spectrum that reflects the measure of disorder in a polymer matrix is known as the disordered longitudinal acoustic mode (D-LAM) and is generally observed below 300 cm^{-1}.[31] Wider bands are indicative of a higher level of disorder in the matrix. In the ormosil without salt, a broad band appears centering around 300 cm^{-1} (not shown). This band may be due to the acoustic vibration mode of the polymeric network. As the salt concentration is increased, this band becomes slightly broader. This indicates the growing disorder of the backbone chains induced by the Mg^{+2}–oxygen interaction. It should be noted that low energy vibrations in inorganic glasses are also referred to as 'Boson bands'.[31c–e] These vibrations generally occur below 100 cm^{-1} and the origin of this band is poorly understood. However, it was proposed that these vibrations are based on quasilocal phonons and the scattering centers for these phonons originate from the broken or strained bonds.[31e] The short-range conformational disorder is also present in these matrices as observed by the changes in the CH_2 stretching modes around 2900 cm^{-1}.

Range 3050–2750 cm^{-1}

This region yields information on the CH_2 stretching vibrations of the matrix. Fig. 2 shows the deconvoluted spectrum for the composition $[2.5]_4[8]$ with $Mg(ClO_4)_2$ salt. The complex nature is clearly observed in the deconvoluted spectra. The bands at around 2950 and 2920 cm^{-1} correspond to the asymmetric CH_2 stretching vibration of the ordered chain conformation (—O-*trans*-C-*gauche*-C-*trans*-O—) and the disordered chain respectively[32] while the band at around 2880 cm^{-1} corresponds to the symmetric CH_2 stretching vibration. The frequencies corresponding to the asymmetric CH_2 stretching modes match with the oligo(ethylene glycol) based matrix[32] reported for

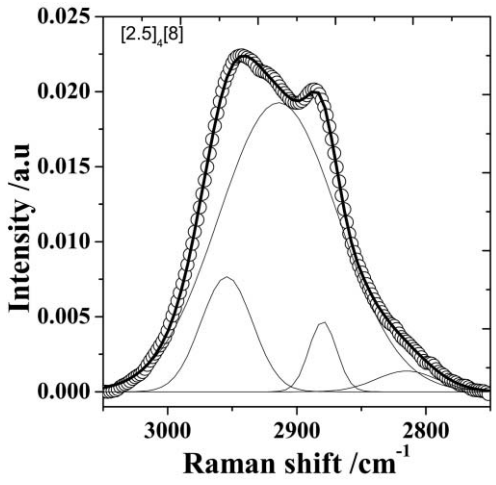

Fig. 2 Deconvolution of the CH_2 stretching bands for the $[2.5]_4[8]$-$Mg(ClO_4)_2$ composition at 25 °C.

Table 2 Ratio of 2918 cm^{-1} to 2955 cm^{-1} band for $[2.5]_4[Y]$-$Mg(ClO_4)_2$ composition with different salt concentrations. The area under each band is calculated from the deconvoluted CH_2 spectra

Composition	Disorder (2918 cm^{-1})/ order (2955 cm^{-1}) ratio
$[2.5]_4[4]$-$Mg(ClO_4)_2$	5.41
$[2.5]_4[8]$-$Mg(ClO_4)_2$	8.14
$[2.5]_4[15]$-$Mg(ClO_4)_2$	8.05
$[2.5]_4[30]$-$Mg(ClO_4)_2$	7.87

lithium based solid electrolytes. Since the present matrix also involves poly(ethylene glycol) units, the two values are taken to be close to 2955 and 2918 cm^{-1} and the spectra are deconvoluted for all the compositions. The deconvolution of the spectra would yield different results if the peak positions are taken to be different. In the present study, proper fit is ascertained based on the lowest χ^2 and highest R^2 values. It is clear from the deconvoluted spectra that the intensity of the disordered band is higher than the intensity of the ordered band. The ratio of the area under the peak of the disordered band to the area under the peak of the ordered band can be considered as a measure of relative population of the disordered to the ordered conformers. This ratio is given in Table 2 for the ormolytes containing $Mg(ClO_4)_2$. It is clear that the disorder increases as a function of salt concentration up to a value of $Y = 8$. When it is further decreased to 4, there is a relative decrease in the level of disorder. This may be attributed to the reduced flexibility and decreased conformational freedom caused by the cations that act as cross-links between the oxygens of neighboring chains.[33] Hence, the system may get stiffer and ordered. The appreciable changes seen in the spectra show that the conformation of the PEG oligomeric network is greatly affected by interactions involving ether oxygens and the magnesium salts. The D-LAM gives the long-range disorder while the CH_2 gives the short-range disorder in the matrix. Both are present to a considerable extent revealing the disordered nature of the TEOS–glycol matrix used in the present studies.

Ion association

The ClO_4^- ion is of tetrahedral (T_d) symmetry with a normal mode of representation $A_1 + E + 2F_2$. Three of these modes that result from the intermolecular vibrations of the perchlorate anions are observed in the present studies. The ν_2 (E) and ν_4 (F_2) modes are deformation modes while the ν_1 (A_1) is a symmetric stretching mode. The deformation modes are observed at 459 cm^{-1} (not shown) and 625 cm^{-1} respectively

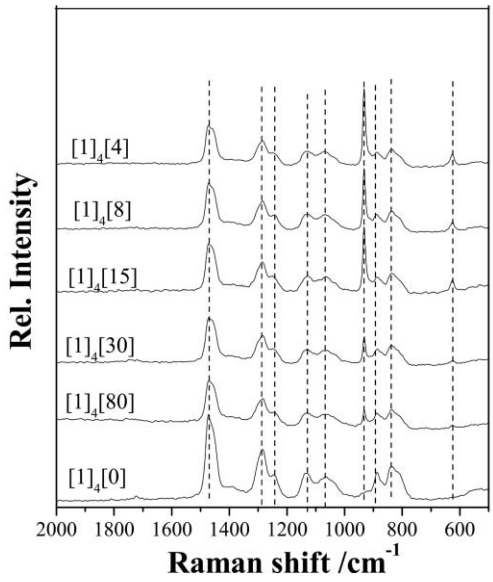

Fig. 3 FT-Raman spectra of ormolytes in the spectral region between 2000–500 cm^{-1} for $[1]_4[Y]$-$Mg(ClO_4)_2$ compositions at 25 °C. The dashed lines indicate the spectral positions at 1468, 1284, 1247, 1126, 1070, 931, 884, 829 and 624 cm^{-1}.

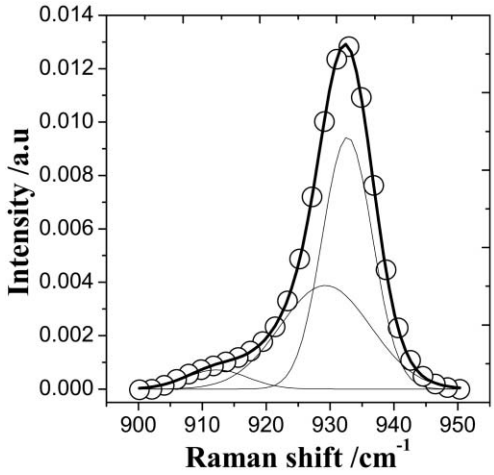

Fig. 4 Deconvoluted ClO_4^- symmetric stretching frequency region for $[2.5]_4[4]$-$Mg(ClO_4)_2$ [0.6 M] at 25 °C.

while the symmetric stretching mode is observed at around 930 cm^{-1} (Fig. 3 and 4). The intensity of the bands corresponding to the deformation modes increases with increasing salt concentration in the matrix. The band at around 930 cm^{-1} shows small changes as a function of concentration of the salt. A splitting of this non-degenerate mode cannot be due to any removal of degeneracy. Hence, the changes in this band are associated with the environment of the anion namely ion association and aggregation effects. Fig. 4 shows the deconvoluted symmetric stretching mode of free ClO_4^- anions. The band at 932 cm^{-1} is assigned to the free ClO_4^- anion. This is similar to the reported value in the case of $LiClO_4$-PPG complexes.[34] The deconvoluted spectra show the development of bands around 910 and 929 cm^{-1}. The 929 cm^{-1} component may be assigned to be due to the ion pair while the 910 cm^{-1} component could be assigned to higher aggregates. Bergstrom and Frech[35] have reported that the ν_s (SO_3) bands from cation coordinated triflate ions are shifted to lower frequencies relative to the 'free triflate ion' when tin and lead triflate salts are used in polypropylene oxide matrices. The observed shift in the frequencies to lower wave numbers has been attributed to the larger interaction of the divalent cations compared to the monovalent ions such as lithium.[36] Similar arguments may be invoked in the present case as well where the divalent magnesium ions interacting with the perchlorate ion leads to a shift in the frequencies to lower wave numbers. Table 3 shows the relative concentrations of the free ion, ion–pair and higher aggregates calculated based on the deconvoluted spectra assuming a single Lorentzian distribution for the total concentration as given in Fig. 4. The salt concentration is given with respect to tetraethylene glycol concentration used. It is clear that the concentrations of ion-pair and the ion aggregates increase while the free ion concentration decreases as a function of salt concentration when the tetraethylene glycol amount used is large in the matrix (*i.e.*) when the *X* ratio is 1 and 2.5. However, when the silicate concentration is larger than the glycol, (*i.e.*) when *X* is 0.5, the concentration of free-ion stays almost constant while the concentration of aggregates shows an increase. The ion-pair however shows a small decrease. The reason for this observation is unclear at present.

Range 2000–500 cm^{-1}

The spectral range 2000–500 cm^{-1} is useful in deciphering information on the chemical nature of the ormolytes. The bands at 1468, 1284 and 1247 cm^{-1} (Fig. 3) are assigned to the $-CH_2$ scissor and the $-CH_2$ twisting modes respectively.[30] The broad bands at 1126 and 1063–1060 cm^{-1} are assigned to C–O stretching/C–C stretching modes while the 1060 cm^{-1} band is due to presence of a $\gamma_{asymmetric}$ (Si–O–Si) mode.[37] The band due to the C–O stretch at 1126 cm^{-1} becomes broad with an increase in the salt concentration. The bands around 830 cm^{-1} are observed in all the cases and are assigned to C–O stretching/CH_2 rocking modes. The presence of all these modes of vibrations confirmed the existence of an oligomeric $-O-CH_2-CH_2$ network.

Nuclear magnetic resonance (NMR) spectroscopy

Solid state ^{29}Si NMR has been used[38] to decipher the silicon environment in the matrix. The ^{29}Si NMR spectrum for $[0.5]_4[30]$–$[MgCl_2]$ is shown in Fig. 5(a). The ormolyte typically displays strong peaks at δ −101.9 and −109.69 ppm with respect to TMS. This is similar to the spectrum observed by Judeinstein and co-workers[15] for a TEOS, PEG matrix. The two peaks are attributed to the $Si\text{-}(OH)_{4-n}O_n$ units where *n* is 3(Q_3) and 4(Q_4) respectively.[38] The Q_2 type of silicon peak is rather weak and is shown at −90.5 ppm. Fig. 5(b) shows the

Table 3 Estimated relative percentage of free anions, ion-pairs and ion-aggregates for different compositions with magnesium perchlorate salts (percentage calculations have been done with respect to free symmetric stretching frequency band, assuming a single Lorentzian shape)

Composition	Salt concentration/M	Percentage of free ions (932 cm^{-1})	Percentage of ion-pairs (~929 cm^{-1})	Percentage of ion-aggregates (~911 cm^{-1})
$[0.5]_4[8]$	0.938	35.14	39.40	1.44
$[0.5]_4[4]$	1.878	35.38	37.23	2.89
$[1.0]_4[8]$	0.7228	45.68	26.40	1.76
$[1.0]_4[4]$	1.4450	39.75	32.89	1.86
$[2.5]_4[8]$	0.2890	44.49	26.50	1.49
$[2.5]_4[4]$	0.578	41.00	30.48	3.80

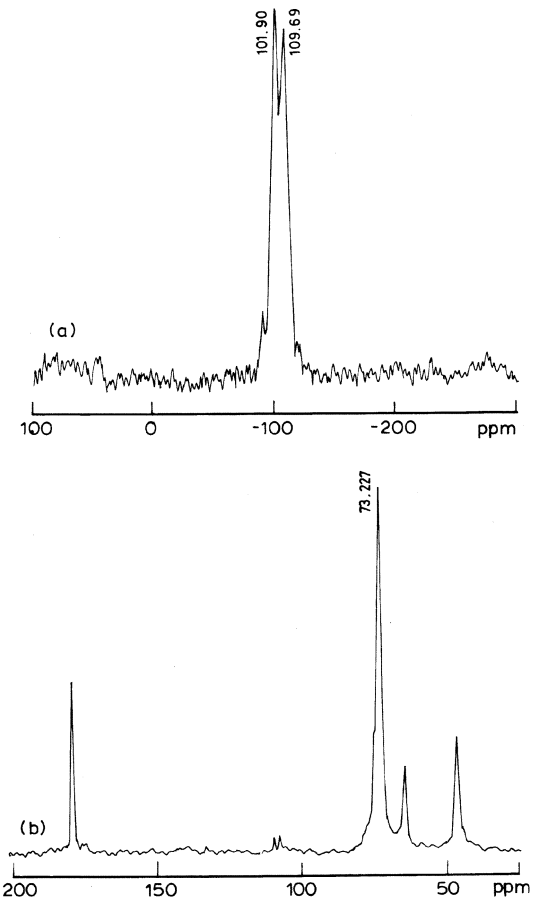

Fig. 5 (a) ^{29}Si MAS-NMR spectra for the $[0.5]_4[30]$-$MgCl_2$ composition and (b) ^{13}C-CP-MAS NMR spectra of the same composition at 27 °C

solid state ^{13}C NMR spectra for the composition $[0.5]_4[30]$–$MgCl_2$. Two intense peaks observed at 73.21 and 64.08 ppm are attributed to the ethylene glycol groups bonded to silicon or silica clusters.[15] The peaks around 46 and 179 ppm correspond to the reference compound, glycine. Lesot and co-workers[39] have recently probed the chemical nature of tetraethoxysilane–tetraethylene glycol composites based on ^{13}C and ^{29}Si NMR spectra. It is revealed that these materials are diphasic where the inorganic aggregates are wrapped around by the organic phase. Additionally, it has been found that the motion of PEG chains are hindered near the silica surface due to hydrogen bonding while the bulk of the PEG phase possesses the properties of the polymer melt.

XRD

X-Ray powder diffractograms (not shown) do not reveal any crystallinity and show only the glassy nature of the matrices. This indirectly points to the dissociation of the salt and further coordination to the matrix leading to an amorphous structure.

Ionic conductivity

Impedance spectroscopy has been used to determine the ionic conductivity of the matrices. The impedance spectra display two distinct relaxation processes, a high frequency relaxation process due to the mobile ion migration in the bulk material and an incomplete low frequency relaxation due to the electrode process like formation of double layer capacitor at the electrode–electrolyte interface. Ionic conductivity is calculated using the relation, $\sigma_I = (L/RA)$ where L is the electrolyte thickness, R is the bulk resistance and A is the area of the electrode. Bulk resistance is calculated from the high frequency intercept of the Z_{img} *vs.* Z_{real} plot. A few heating–cooling cycles between ambient to 90 °C were performed before the experiment. The conductivity of pure matrices without salt have been determined and the values work out to be 10^{-9} and 10^{-8} S cm^{-1} for the $[0.5]_4[0]$ and $[2.5]_4[0]$ compositions, respectively, at 25 °C. The conductivities of the salt-rich matrices are, however, of the order of 10^{-5} S cm^{-1} at ambient temperatures. Hence, it may be concluded that the major contribution to the ionic conductivity arises due to the incorporated salt. At this point, it should be emphasized that Dunn and co-workers[14] reported that water could be completely eliminated from the sol–gel silicate based lithium ionic conductors and the ionic contribution is solely from the metallic salt incorporated in the matrix. Dunn *et al.* also reported that the protonic conductivity decreased substantially when the solvent is removed from the sol–gel matrices.[40] It is shown in the present study, that the residual water molecules are coordinated with the glycol matrix and the salt based on IR measurements given earlier. It is of interest to note that we have fabricated supercapacitors based on these solid electrolytes that yield a working voltage of 3 V for 10^3 cycles at 80 °C. This is not possible if loosely bound water molecules and protons are present in the matrix. Hence, we believe that the ionic conductivity observed in the composites is largely due to the incorporated metal salts in the matrix.

Fig. 6 represents the variation of ionic conductivity as a function of temperature for selected ormolyte compositions containing $MgCl_2$ and $Mg(ClO_4)_2$ salts. The temperature dependence of the conductivity of gel electrolytes is approximated by a free volume model (VTF) behaviour as the conductivity is influenced by the glass transition temperature of the matrix.[15] In the present case as well, the temperature dependence of conductivity may follow a VTF behaviour since the electrolyte is gel-like containing poly(ethylene glycol) as the plasticizer. The glass transition temperature (T_g) for the poly(ethylene glycol)–silicate composites is reported to be

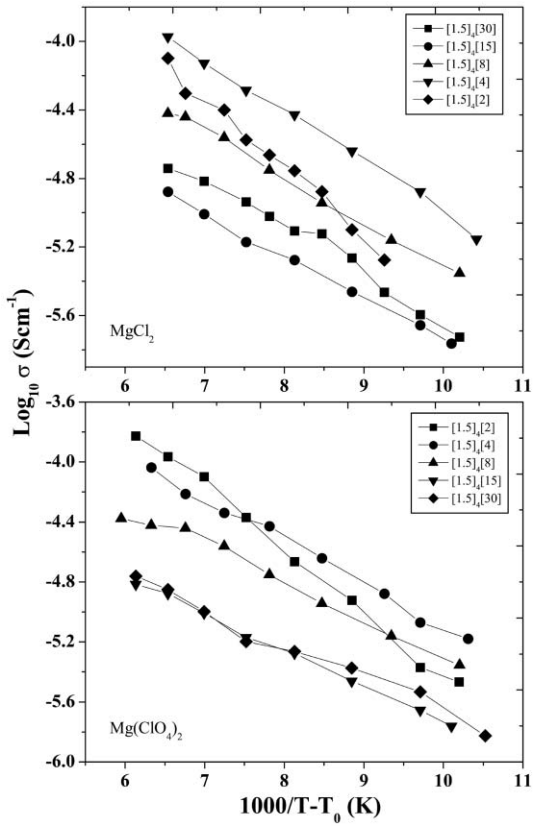

Fig. 6 Temperature dependence (VTF; T_0 = 200 K) of ionic conductivity for (a) $[1.5]_4[Y]$-$MgCl_2$ and (b) $[1.5]_4[Y]$-$Mg(ClO_4)_2$ compositions in the temperature range between 25–80 °C. The solid lines are only guidelines to the eye.

−70 °C.[15] In the present studies, the temperature dependence of conductivity is represented in Fig. 6 using the same T_g of −70 °C and it is inferred that the PEG–silicate matrix deviates from a pure VTF behaviour. This is similar to the reported trend of ethylene glycol–silicate based matrices for lithium ion containing solid electrolytes.[15] The apparent activation energy determined based on a linear fit of log (conductivity) versus $1/T$, in the range 25–65 °C, works out to be of the order of 0.4 eV. These values are higher than the observed values for polymeric or composite electrolytes[21,41] but can be compared with systems where large anions are complexed with the matrix. Generally the activation energy for ionic conduction involves ion–ion interaction energy, ion–polymer interaction energy and the energy of formation of free volume for ion movement.[5] In the present case, one additional interaction energy between segmental motion of the ethylene oxide units and the inorganic silica domains should also be included.

The lower conductivity of the $MgCl_2$ incorporated composite may be due to the high lattice energy (2326 kJ mol^{-1}) of the salt which would result in the ionization being relatively lower. It has been reported that alkali metal salts with lattice energies higher than certain values are not able to form complexes with PEO.[42] However, Armand[28] reported that salts having large anions like I^-, ClO_4^- and $CF_3SO_3^-$ *etc.* can overcome this difficulty. It should, however, be pointed out that there was no evidence of free $MgCl_2$ salt in the matrix from XRD data. Hence, the lattice energy being high may not be directly responsible for the observed decrease in conductivity. The conductivity data show a value of 10^{-7} S cm^{-1} for the composition $[0.5]_4[Y][MgCl_2]$ while the corresponding conductivity of the magnesium perchlorate incorporated matrix is 10^{-5} S cm^{-1} at room temperature. The ionic conductivity depends on the number and the mobility of charge carriers present in the matrix. The reasons for the lower conductivity in the case of the $MgCl_2$ incorporated matrix may be due to both reasons given above. The small size of the chloride ion may lead to a larger interaction with the magnesium ion present in the matrix leading to a lower mobility. It is to be emphasized that both $MgCl_2$ and $Mg(ClO_4)_2$ salts fully dissolve when TEOS/M^{n+} = 2 when the PEG/TEOS ratio is 2.5 while they do not dissolve completely when the PEG/TEOS ratio is 0.5. This clearly indicates that the solvation power of the matrix increases with increasing ethylene oxide units.

Summary

Magnesium based SiO_2-$(PEG)_4$-MgX_2 organic–inorganic composites have been successfully synthesized in the form of transparent monoliths, by a sol–gel process. The salts are found to be dissociated and mostly solvated into $(PEG)_4$ phase. FT-IR and FT-Raman studies indicate the coordination of divalent metal ions with ether oxygen of the matrix. The electrical conductivity of the solid electrolytes is of the order of $\sim 10^{-5}$ S cm^{-1} at 25 °C and it reaches $\sim 10^{-3}$ S cm^{-1} at 80 °C. The conductivity data follows VTF behavior. The activation energies are of the order of 0.4 eV in the temperature range 65–85 °C. NMR experiments reveal information about the silicon and carbon environment at the molecular scale. The solid electrolytes are currently being used for double-layer capacitor applications and studies are underway.

Acknowledgement

We thank the Ministry of Non-conventional Energy Sources, New Delhi, India for financial assistance. The NMR spectra were recorded at SIF, IISc. with the help of Mr. Willson. The authors also appreciate the assistance of A. Roychoudhury in carrying out XRD measurements.

References

1 T. D. Gregory, R. J. Hoffman and R. C. Winterton, *J. Electrochem. Soc.*, 1990, **137**, 775.
2 P. Novak, R. Imhof and O. Hass, *Electrochim. Acta*, 1999, **45**, 351.
3 D. Aurbach, Z. Lu, A. Schechter, Y. Gofer, H. Gizbar, R. Turgeman, Y. Cohen, M. Moshkovich and E. Levi, *Nature*, 2000, **407**, 724.
4 L. L. Yang, R. Hug and G. C. Farrington, *Solid State Ionics*, 1986, **18**, 291.
5 R. Hug, G. Chiodelli, P. Ferloni, A. Magistris and G. C. Farrington, *J. Electrochem. Soc.*, 1988, **135**, 524.
6 K. C. Andrews, M. Cole, R. J. Latham, R. G. Linford, H. M. Williams and B. R. Dobson, *Solid State Ionics*, 1988, **28**, 929.
7 G. Girish Kumar and N. Munichandraiah, *Solid State Ionics*, 2000, **128**, 203.
8 S. Ikeda, Y. Mori, Y. Furuhashi, H. Masuda and O. Yamamoto, *J. Power Sources*, 1999, **81–82**, 720.
9 N. Yoshimoto, Y. Tomonaga, M. Ishikawa and M. Morita, *Electrochim. Acta*, 2001, **46**, 1195.
10 L. L. Yang, A. R. McGhie and G. C. Farrington, *J. Electrochem. Soc.*, 1986, **133**, 1380.
11 A. G. Martins and C. A. C. Sequeira, *J. Power Sources*, 1990, **32**, 107.
12 A. Patrick, M. Giasse, R. Latham and R. Linford, *Solid State Ionics*, 1986, **18–19**, 1063.
13 J. L. Acosta and E. Morales, *Electrochim. Acta*, 1998, **43**, 791.
14 P. U. Wu, S. R. Holm, A. T. Doung, B. Dunn and R. B. Kaner, *Chem. Mater.*, 1997, **9**, 1004.
15 P. Judeinstein, J. Titman, M. Stamm and H. Schmidt, *Chem. Mater.*, 1994, **6**, 127.
16 B. Wang, S.-P. Szu, M. Tsai, M. Greenblatt and L. C. Klein, *Chem. Mater.*, 1992, **4**, 191.
17 O. Lev, Z. Wu, S. Bharati, V. Glezer, A. Modestov, J. Gun, L. Rabinovich and S. Sampath, *Chem. Mater.*, 1997, **9**, 2354.
18 B. Wang, S-P. Szu, M. Greenblatt and L. C. Klein, *Solid State Ionics*, 1991, **48**, 297.
19 M. Tsai, S.-P. Szu, B. Wang and M. Greenblatt, *J. Non-Cryst. Solids*, 1991, **136**, 227.
20 S.-P. Szu, M. Greenblatt and L. C. Klein, *Solid State Ionics*, 1991, **46**, 291.
21 P. Judeinstein, J. Livage, A. Zarudiansky and R. Rose, *Solid State Ionics*, 1988, **28–30**, 1722.
22 J. Wen and G. L. Wilkes, *Chem. Mater.*, 1996, **8**, 1667.
23 L. Depre, J. Kappel and M. Popall, *Electrochim. Acta*, 1998, **43**, 1301.
24 G. B. Croce, L. Appetechi, B. Perci and B. Scrosati, *Nature*, 1998, **394**, 456.
25 D. Ravaine, A. Seminet, Y. Charbonillit and M. Vincens, *J. Non-Cryst. Solids*, 1986, **82**, 210.
26 (*a*) O. Dag, A. Verma, G. A. Ozin and C. T. Kresge, *J. Mater. Chem.*, 1999, **9**, 1475; (*b*) C. M. Nilson, T. J. Bonagamba, H. Panepneci, K. Dahmouche, P. Judeinstein and M. A. Aegester, *Macromolecules*, 2000, **33**, 1280.
27 P. Judeinstein and C. Sanchez, *J. Mater. Chem.*, 1996, **6**, 511–525.
28 M. Armand, *Solid State Ionics*, 1983, **9–10**, 745.
29 P. A. Buining, B. M. Humbel, A. P. Phillose and A. J. Verkleji, *Langmuir*, 1997, **13**, 3921.
30 K. Horikoshi, K. Hata, N. Kawabata and S.-Ichi. Ikawa, *J. Mol. Struct.*, 1990, **239**, 33.
31 (*a*) R. G. Snyder, *J. Chem. Phys.*, 1982, **76**, 3921; (*b*) R. G. Snyder and S. L. Wunder, *Macromolecules*, 1986, **19**, 496; (*c*) R. M. Almeida, *J. Non-Cryst. Solids*, 1988, **106**, 347; (*d*) A. P. Sokolov, A. Kisluik, M. Soltwisch and D. Quitman, *Phys. Rev. Lett.*, 1992, **69**, 1540; (*e*) V. K. Tikhomirov, L. F. Santos, R. M. Almeida, A. Jha, J. Kobelke and M. Scheffler, *J. Non-Cryst. Solids*, 2001, **284**, 198.
32 S. Shashikov, S. Wartewig, B. Sandner and J. Tubke, *Solid State Ionics*, 1996, **90**, 261.
33 (*a*) S. Schantz, *J. Chem. Phys*, 1991, **94**, 6296; (*b*) S. Schantz, L. M. Torell and R. Stevens, *J. Chem. Phys.*, 1991, **94**, 6862.
34 S. Schantz, L. M. Torell and J. R. Stevens, *J. Appl. Phys.*, 1988, **64**, 2038.
35 (*a*) P.-A. Bergstrom and R. Frech, *J. Phys. Chem.*, 1995, **99**, 12603; (*b*) A. Bernson, J. Lindgren, W. Huang and R. Frech, *Polymer*, 1995, **36**, 4471.
36 (*a*) P. G. Shridhar, H. Kersti, T. Jorgen and L. Jan, *J. Phys. Chem.*, 1993, **97**, 11402; (*b*) J. Manning and R. Frech, *Polymer*, 1992, **33**, 3487.
37 X. Li and T. A. King, *J. Non-Cryst. Solids*, 1996, **204**, 235.

38 (*a*) G. E. Maciel and D. W. Sindorf, *J. Am.Chem. Soc.*, 1980, **102**, 7606; (*b*) K. A. Smith, R. J. Kirkpatrick, E. Oldfield and D. M. Henderson, *Am. Mineral.*, 1983, **68**, 1206.
39 P. Lesot, S. Chapuis, J.-P. Bayle, J. Rault, E. Lafontaine, A. Campero and P. Judeinstein, *J. Mater. Chem.*, 1998, **8**, 147.
40 H. Durakpasa, M. W. Breiter and B. Dunn, *Electrochim. Acta*, 1993, **38**, 371.
41 (*a*) Y. Charbouillot, D. Ravaine, M. Armand and C. Poinsignon, *J. Non-Cryst. Solids*, 1988, **103**, 325; (*b*) M. Armand, *Adv. Mater.*, 1990, **2**, 278.
42 R. Frech, *Solid State Ionics*, 1996, **92**, 151.